

Observation of photoinduced phase transition in phase-separated $\text{Pr}_{0.55}(\text{Ca}_{1-y}\text{Sr}_y)_{0.45}\text{MnO}_3$ thin films via x-ray photoemission spectroscopy

K. Takubo, J.-Y. Son, and T. Mizokawa

*Department of Physics and Department of Complexity Science and Engineering,
University of Tokyo, 5-1-5 Kashiwanoha, Chiba 277-8581, Japan*

N. Takubo and K. Miyano

*Research Center for Advanced Science and Technology (RCAST),
University of Tokyo, Tokyo 153-8904, Japan*

(Dated: August 24, 2021)

Abstract

Perovskite manganite thin films, $\text{Pr}_{0.55}(\text{Ca}_{1-y}\text{Sr}_y)_{0.45}\text{MnO}_3$, have been studied using x-ray photoemission spectroscopy in order to clarify the consequence of the competition between ferromagnetic metal (FM) and charge-orbital ordered insulator (COOI). Films with $y = 0.40$ undergo uniform paramagnetic insulator to FM transition. On the other hand, in films with $y = 0.25$, the composition near the bicritical point, phase separation of COOI and FM domains is indicated by the spectral change below 125 K. Interestingly, between 50 K and 70 K, the visible laser illumination transfers the COOI-like spectra obtained in cooling process to the FM-like spectra obtained in warming process. This indicates that the photoinduced IMT is governed by the increase of the FM volume fraction and is deeply related to the phase separation between the FM and COOI states.

PACS numbers: 79.60.-i, 71.30.+h, 75.47.Gk, 71.27.+a

Photoinduced phase transition (PIPT) has recently attracted considerable attention. A wide variety of PIPT has been reported such as the spin transition in iron complexes [1], magnetization in cobalt-iron cyanides [2], valence transition in $\text{Cs}_2\text{Au}_2\text{Br}_6$ [3], order to disorder phase transition in InSb [4, 5], insulator to metal transition (IMT) in $(\text{EDO-TTF})_2\text{PF}_6$ [6] and VO_2 [7], and so on. Among them, photoinduced IMT in perovskite manganites is unique in that despite the orders of magnitude resistance drop as a result of photo-irradiation, it has been indicated that the resulting conduction path is only filamentary [8]. This is in line with the proposal of the colossal magnetoresistance (CMR) at low temperatures being percolative phenomena in a metal-insulator mixed state; a relatively small magnetic field can cause enormous resistance drop simply because the magnetic field needs to destroy only small fraction of intervening insulating phase between metallic islands. This is the scenario called CMR1 [9].

Although the phenomenon is very clear superficially, the role the photoexcitation plays in the IMT is not clear at all. Let us recall that the ‘evidences’ of the photoinduced IMT in manganites so far are the macroscopic conductivity jump [8, 10] and the increase in the magnetization [11], none of which proves that the new photoinduced phase is indeed metallic. It should be pointed out that simple photoinduced redistribution or coalescence of metallic islands can establish connectivity of metallic phase in a two-phase coexisting state. A ferromagnetic state can well be insulating in manganites [12].

In order to clarify these questions, we performed x-ray photoemission spectroscopy (XPS) measurements on manganite thin films under photo-irradiation. By observing the electronic density of states, we found the first direct evidence of the photoinduced metallic phase. The PIPT, however, occurs only within a hysteresis loop with a clear temperature cutoff. This indicates that the presence of competing orders separated by a first-order phase transition in the vicinity of a multicritical point is essential for the PIPT. The two distinct ordered states need not be coexisting before photo-irradiation, unlike the CMR1 scenario, but the parameter space for the true PIPT is rather small, which conforms to our experience that the photoinduced IMT is limited to a small class of manganites.

Thin films of $\text{Pr}_{0.55}(\text{Ca}_{1-y}\text{Sr}_y)_{0.45}\text{MnO}_3$ (PCSMO) coherently grown on $(\text{LaAlO}_3)_{0.3}(\text{SrAl}_{0.5}\text{Ta}_{0.5}\text{O}_3)_{0.7}$ (LSAT) (011) substrate have been employed as an archetypal example [10]. The thickness is about 80 nm. Two compositions ($y = 0.25$ and 0.40) were chosen. The $y = 0.40$ sample shows simple paramagnetic insulator (PI) to ferromagnetic

metal (FM) transition on cooling while the $y = 0.25$ sample is located near a bicritical point and undergoes PI to charge-orbital ordered insulator (COOI) transition followed by a transition to FM. The photoemission spectroscopy has been performed using a JPS9200 spectrometer equipped with a monochromatized AlK α x-ray source ($h\nu = 1486.6$ eV). The total resolution was ~ 0.6 eV. The pressure of the spectrometer was $\sim 1 \times 10^{-7}$ Pa during the measurement. The thermal cycles of XPS measurements were performed repeatedly to confirm reproducibility. A Nd:YAG pulsed laser provided optical excitation of 2.3 eV (532 nm) at a repetition rate of 30 Hz with the pulse width of 10 ns. The energy per pulse was 1.0 mJ and the beam diameter was about 4 mm corresponding to the density of $1.7 \times 10^{16} \text{cm}^{-2}$ photons per pulse.

Figure 1 shows the (a) Mn $2p_{3/2}$ and (b) valence-band spectra of $y = 0.40$ film. The spectra are normalized to the integrated intensities from 636.0 eV to 648.0 eV for the Mn $2p_{3/2}$ and from -1.0 eV to 4.0 eV for the valence-band, respectively. The PI to FM transition occurs at ~ 200 K [inset of Fig. 1 (a)]. The XPS data show dramatic change in going from PI to FM. While the Mn $2p_{3/2}$ spectrum of the PI (~ 300 K) has only the poorly-screened feature (~ 641 eV), the spectrum of the FM (~ 20 K) additionally has the well-screened feature at the lower binding energy side (~ 639 eV) due to the Mn $3d$ carriers. The well-screened feature reflects the core-hole screening through the density of states at the Fermi level [$D(E_F)$][14, 15]. This is in accordance with the weight enhancement of $D(E_F)$ (structure A) through the weight transfer from structure B (~ 1.0 eV) in the valence band spectra with decreasing temperature (Fig. 1 (b)). Structures A and B are the coherent and incoherent bands of the Mn $3d$ e_g states, while the Mn $3d$ t_{2g} and Pr $4f$ states sit around ~ 2 eV (structure C)[16, 17]. The obvious enhancement of $D(E_F)$ in the metallic phase suggests three-dimensional metallic character.

Figure 2 (a) gives the Mn $2p_{3/2}$ XPS data of $y = 0.25$ film. The spectra are normalized in the same way as for $y = 0.40$. Although the well-screened structure of Mn $2p_{3/2}$ (~ 639 eV) for $y = 0.25$ also appears at low temperature, it is weaker compared to $y = 0.40$. For the quantitative evaluation, the integrated intensity from 638.0 eV to 640.0 eV, namely, the area of the well-screened feature, is plotted against temperature in Fig. 2 (b) for both $y = 0.40$ and 0.25 . For $y = 0.40$, in the cooling process, the integrated intensity (green closed squares) starts to increase at the IMT temperature (~ 200 K) of the resistance. The onset of integrated intensity matches the resistance drop, indicating that the PI to FM transition

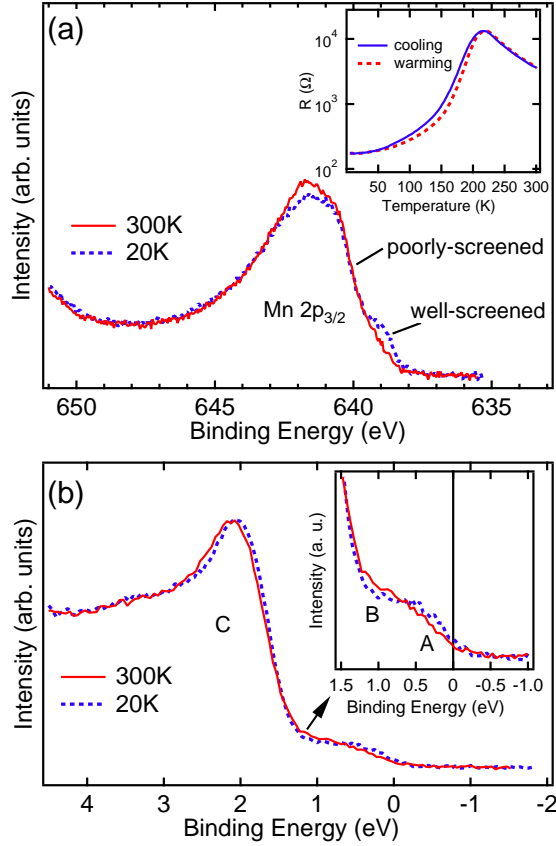


FIG. 1: (Color online). (a) Mn $2p_{3/2}$ and (b) valence-band XPS data of PCSMO ($y = 0.40$) thin film at 35 K and 300 K. The inset of the upper panel shows the resistance of the film.

takes place uniformly and no phase separation appears in the film.

However, for $y = 0.25$ there is a discrepancy between the temperature dependence of the integrated intensity and that of the resistance. In the cooling process, although the integrated intensity gradually increases below 125 K (blue closed triangles), the resistance keeps increasing down to ~ 67 K. This indicates that the FM domains start to appear in the COOI phase below 125 K in the cooling process. On the other hand, in the warming process (red open circles) the integrated intensity gradually decreases above 50 K but the resistance stays at the low metallic value up to 110 K. This suggests that the COOI domains start to grow in the metallic phase. Moreover there is a distinct thermal hysteresis between the cooling and warming curves of the integrated intensity. The hysteretic temperature region is thus also characterized by the two-phase coexistence of FM and COOI, similar to the previous report about $\text{La}_{1-x-y}\text{Pr}_y\text{Ca}_x\text{MnO}_3$ in Ref. 18. Because the small temperature

dependence of $D(E_F)$ within the FM phase[15, 19] caused by improvement of spin alignment in the double exchange regime is almost saturated far below T_C , the area of the well-screened feature is interpreted to be proportional to the volume of the FM state.

The difference in the temperature dependence for $y = 0.40$ and 0.25 is understood by inspecting the phase diagram (inset of Fig. 2(b)). With decreasing temperature, the $y = 0.25$ film crosses a first-order phase boundary between the COOI and FM. A small fraction of FM appears at $\sim 125\text{K}$ followed by a gradual growth, which is completely masked in the macroscopic resistance measurements by the resistivity increase of the insulating part as the temperature is lowered. When the FM fraction reaches a threshold for establishing a continuous path, the resistance drops abruptly. On warming, the reverse process occurs for the insulating phase in the metallic background. If this were to be a simple percolation problem, the threshold should be around 0.6 for the metal phase fraction x_M [20]. However, x_M is estimated to be about 0.6 even at 20K, assuming that x_M at the same temperature is unity for $y = 0.40$. Therefore, a simple percolation theory is not applicable here. However, it should be noted that the threshold x_M is about 0.3 - 0.4 both for cooling and warming runs. This may hint a presence of some texture in the FM-COOI mixed state not affected by the thermal cycling.

These observations are also consistent with the behavior of the valence-band spectra (Fig.3). Comparing the metallic state (25 K) to the insulating state (300 K, 150 K), the weight transfer from structure B to structure A is observed crossing the IMT. The spectra at 150 K have a larger band gap (~ 0.3 eV) than those at 300 K, reflecting the COOI nature at 150 K. Moreover the spectra at 70 K in cooling process have smaller $D(E_F)$ compared to the spectra in the warming process.

To study the photoinduced change of the film, the XPS data were taken for $y = 0.25$ before and after visible light irradiation at 50 K, 60 K, 70 K, 80K, and 85 K. More than 1000 laser pulses were shone on the sample. The photoinduced effect in the integrated intensity is superposed on the thermal hysteresis in Fig. 4 (a). The arrows denote the changes caused by the laser irradiation. Two features are worth noting; (1) the laser-irradiation induces clear IMT only below a critical temperature (around 75K) and (2) the resulting metallic state is identical to that reached in the warming run at the respective temperatures [see also the insets of Fig. 4]. This transition is persistent as long as the temperature is held constant and can be reversed by heating above 120K as previously reported [10]. In contrast, the laser

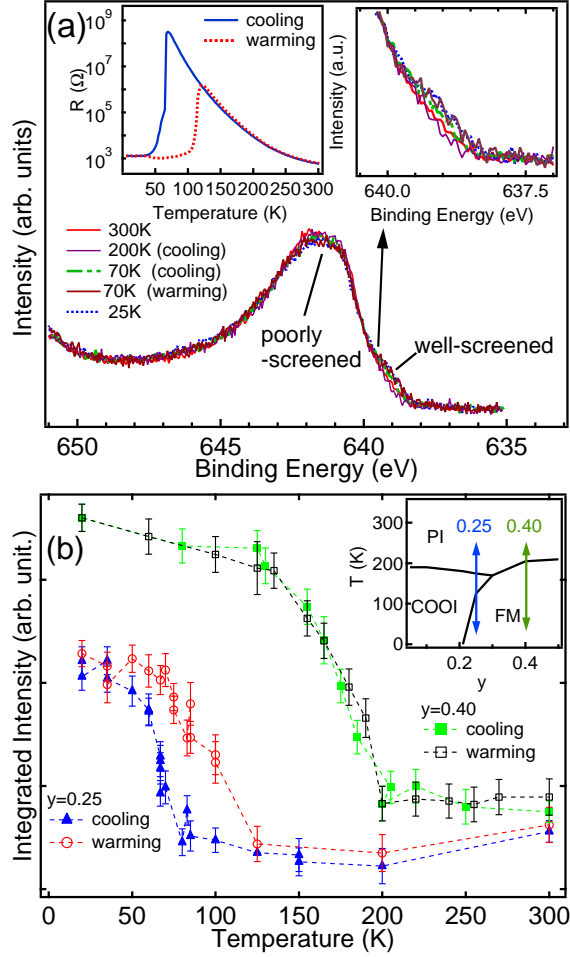


FIG. 2: (Color online). (a) Mn $2p_{3/2}$ XPS data of PCSMO ($y = 0.25$) thin film at various temperatures. The left inset shows the resistance of the film. In the right inset, the spectra of the well-screened feature are expanded. (b) Temperature dependence of the integrated intensity from 638.0 eV to 640.0 eV for the PCSMO XPS data. The (blue) closed triangles and (red) open circles indicate the cooling and warming process for $y = 0.25$, respectively. The (green) closed squares show the plots for $y = 0.40$. The inset of lower panel shows the phase diagram of PCSMO.

illumination effect for $y = 0.40$ has not been observed in all temperature range, including the insulating state.

It is clear that the PIPT in PCSMO is due to the crossing of a first-order phase transition line below a bicritical point (inset, Fig. 2(b)). The true phase transition point is near 75K but the system apparently can be supercooled as much as 50K. The photoirradiation induces charge-orbital disordered state by charge transfer excitation, tipping the balance momen-

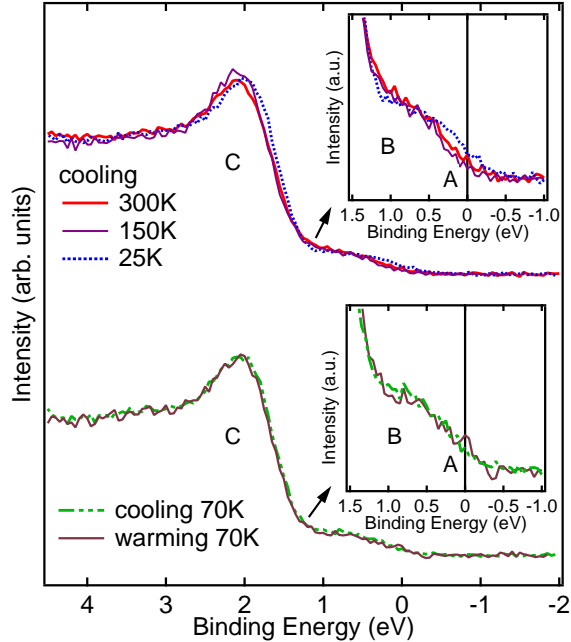


FIG. 3: (Color online). Valence-band XPS data of PCSMO ($y = 0.25$) thin film at various temperatures.

tarily to FM. The system subsequently falls back to COOI above 75K but it is transformed to FM below. With sufficient laser pulses, the metal volume fraction thus formed is as much as allowed by the equilibrium condition at the temperature. The PIPT is thus acting on the volume of COOI and the presence of the metal islands close to the percolation limit is not a prerequisite for the drastic resistance drop under the photoexcitation. Even below this critical temperature, however, a considerable amount of photon density is necessary for the transformation to take place [10]. Together with the extreme stability of the superheated or supercooled states, it is obvious that the COOI and FM are separated by a large energy barrier associated with a long range order not easily destroyed by a single particle excitation by photons.

An obvious candidate for such an order is elastic deformation. The coupling to the Jahn-Teller type lattice distortion stabilizes the COOI considerably while the FM is deformation free. Because the distortion is collective and the elastic interaction is long range, the difficulty in overcoming the barrier is clear, resulting in the large hysteresis. The analogy to the martensitic transformation has been pointed out [21]. Indeed, x-ray diffraction shows that there is no structural change at the PI to FM transition for the $y = 0.40$ film while the PI

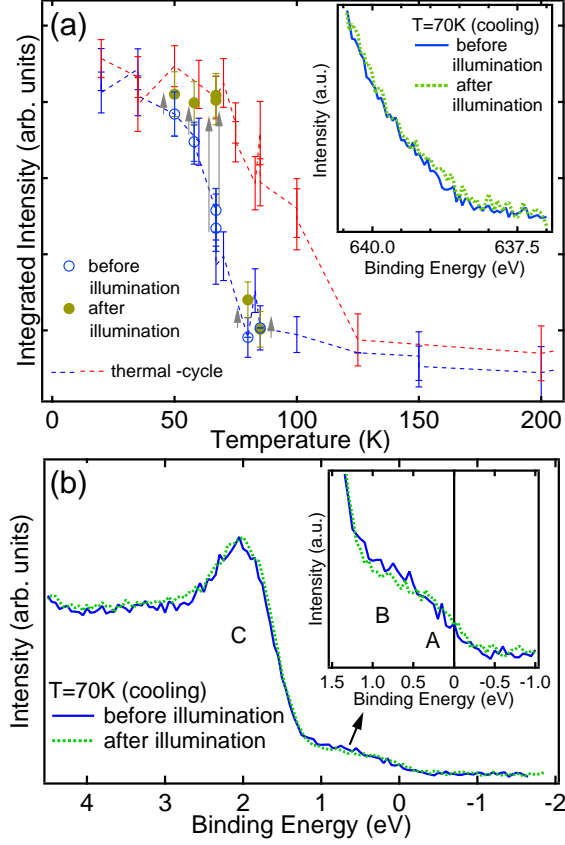


FIG. 4: (Color online). (a) Integrated intensity from 638.0 eV to 640.0 eV of the XPS data for $y = 0.25$ before and after laser illumination superposed on the temperature dependence. The arrows denote the changes caused by the laser illumination. The inset shows the spectra for $y = 0.25$ at 70 K before and after the laser illumination. (b) Valence-band XPS data for $y = 0.25$ at 70 K before and after laser illumination.

to COOI transformation for $y = 0.25$ film is accompanied by a lattice deformation [22]. It is to be noted that the $y = 0.25$ film is not 100% FM even at the lowest temperature. The robustness of the COOI phase in $y = 0.25$ sample is peculiar to this composition but not due to the film being inherently nonuniform. This is clear by the sharp transition in the $y = 0.40$ film.

In conclusion, we have studied the electronic structure of PCSMO ($y = 0.25, 0.40$) thin films by means of XPS. In the case of $y = 0.40$, the IMT is clearly observed on the Mn $2p$ core-level and valence-band spectra across the PI to FM transition. For $y = 0.25$, hysteresis is observed between 50 K and 125 K associated with the COOI-FM first-order phase transition. It is phase separated below 125 K and does not reach 100% FM even at the

lowest temperature. Persistent PIPT from COOI to FM is also observed for $y = 0.25$ in the temperature range between 50 K and 70 K. After sufficient illumination, the system is as much metallic as allowed in the equilibrium, showing that the photons transform the bulk of COOI rather than connect the marginally disconnected metallic islands as is proposed for CMR1.

The authors would like to acknowledge fruitful discussions with G. A. Sawatzky. This work was supported by Grant-In-Aid for Scientific Research (17105002, 16684010, 16204024, 16076207, 15104006) from the Japan Society for the Promotion of Science.

-
- [1] S. Decurtins *et al.*, Chem. Phys. Lett. **105**, 1 (1984).
 - [2] O. Sato *et al.*, Science **272**, 704 (1996).
 - [3] X. J. Liu *et al.*, Phys. Rev. B **61**, 20 (2000).
 - [4] A. M. Lindenberg *et al.*, Phys. Rev. Lett. **84**, 111 (2000).
 - [5] K. Sokolowski-Tinten *et al.*, Nature **422**, 287 (2003).
 - [6] M. Chollet *et al.*, Science **307**, 86 (2005).
 - [7] A. Cavalleri *et al.*, Phys. Rev. Lett. **87**, 237401 (2001).
 - [8] K. Miyano *et al.*, Phys. Rev. Lett. **78**, 4257 (1997) and M. Fiebig *et al.*, Science **280**, 1925 (1998).
 - [9] H. Aliaga *et al.*, Phys. Rev. B **68**, 104405 (2003).
 - [10] N. Takubo *et al.*, Phys. Rev. Lett. **95**, 017404 (2005).
 - [11] Y. Okimoto *et al.*, Appl. Phys. Lett. **80**, 1031 (2002).
 - [12] Y. Endoh *et al.*, Phys. Rev. Lett. **82**, 4328 (1999).
 - [13] Y. Tomioka and Y. Tokura, Phys. Rev. B **66**, 104416 (2002).
 - [14] K. Horiba *et al.*, Phys. Rev. Lett. **93**, 236401 (2004).
 - [15] H. Tanaka *et al.*, Phys. Rev. B **73**, 094403 (2006).
 - [16] A. Chainani *et al.*, Phys. Rev. B **56**, R15513 (1997).
 - [17] A. Sekiyama *et al.*, Phys. Rev. B **59**, 15528 (1999).
 - [18] D. D. Sarma *et al.*, Phys. Rev. Lett. **93**, 097202 (2004).
 - [19] J.-H. Park *et al.*, Phys. Rev. Lett. **76**, 4215 (1996).
 - [20] B. J. Last and D. J. Thouless, Phys. Rev. Lett. **27**, 1719 (1971).

- [21] V. Podzorov *et al.*, Phys. Rev. B**64**, 140406(R) (2001).
- [22] Y. Wakabayashi - private communication.